Microbial mechanisms and ecosystem flux estimation for aerobic NO$_y$ emissions from deciduous forest soils

Ryan M. Mushinski[a,b,c,1], Richard P. Phillips[a], Zachary C. Payne[d], Rebecca B. Abney[c], Insu Jo[e], Songlin Fei[e], Sally E. Pusede[f], Jeffrey R. White[b,c], Douglas B. Rusch[g], and Jonathan D. Raff[b,c,d,1]

[a]Department of Biology, Indiana University, Bloomington, IN 47405; [b]Integrated Program in the Environment, Indiana University, Bloomington, IN 47405; [c]School of Public and Environmental Affairs, Indiana University, Bloomington, IN 47405; [d]Department of Chemistry, Indiana University, Bloomington, IN 47405; [e]Department of Forestry and Natural Resources, Purdue University, West Lafayette, IN 47907; [f]Department of Environmental Sciences, University of Virginia, Charlottesville, VA 22903; and [g]Center for Genomics and Bioinformatics, Indiana University, Bloomington, IN 47405

Reactive nitrogen oxides (NO$_y$; NO$_y$ = NO + NO$_2$ + HONO) decrease air quality and impact radiative forcing, yet the factors responsible for their emission from nonpoint sources (i.e., soils) remain poorly understood. We investigated the factors that control the production of aerobic NO$_y$ in forest soils using molecular techniques, process-based assays, and inhibitor experiments. We subsequently used these data to identify hotspots for gas emissions across forests of the eastern United States. Here, we show that nitrogen oxide soil emissions are mediated by microbial community structure (e.g., ammonium oxidizer abundances), soil chemical characteristics (pH and C:N), and nitrogen (N) transformation rates (net nitrification). We find that, while nitrification rates are controlled primarily by chemoautotrophic ammonia-oxidizing archaea (AOA), the production of NO$_y$ is mediated in large part by chemoautotrophic ammonia-oxidizing bacteria (AOB). Variation in nitrification rates and nitrogen oxide emissions tracked variation in forest communities, as stands dominated by arbuscular mycorrhizal (AM) trees had greater N transformation rates and NO$_y$ fluxes than stands dominated by ectomycorrhizal (ECM) trees. Given mapped distributions of AM and ECM trees from 78,000 forest inventory plots, we estimate that broadleaf forests of the Midwest and the eastern United States as well as the Mississippi River corridor may be considered hotspots of biogenic NO$_y$ emissions. Together, our results greatly improve our understanding of NO$_y$ fluxes from forests, which should lead to improved predictions about the atmospheric consequences of tree species shifts owing to land management and climate change.

nitrification | deciduous forests | soil emissions | nitric oxide | nitrous acid

Decreases in anthropogenic nitrogen oxide emissions and rises in fertilizer use and global temperatures have increased the relative importance of soil emissions to the global reactive nitrogen oxide [NO$_y$; NO$_y$ = nitric oxide (NO), NO$_2$, nitrous acid (HONO)] budget (1). While soil emissions of nitrogen oxides associated with agriculture are well studied (2), far less is known about the sources and sinks of these gases within forests (3), which cover ~31% of Earth's surface. Uncertainties in the mechanisms associated with soil–atmospheric exchange of NO$_y$ within forests limit our ability to model atmospheric composition and predict how nitrogen (N)-cycle processes influence ozone, aerosols, and climate. To advance modeling efforts of these nitrogen oxides, a better understanding is needed of what properties control their emission.

It is well established that NO$_y$ are released during the process of nitrification (Fig. 1), which is the microbiological conversion of ammonia (NH$_3$) to nitrate (NO$_3^-$). Nitrification is one of the most important steps in the global N cycle (4) in that it facilitates both the availability of N to plants and microbes and the degree to which ecosystems lose N via leaching (terrestrial ecosystems) and gaseous losses (both terrestrial and aquatic ecosystems). Most of the N transformations that occur during nitrification are mediated by autotrophic microbes. The initial step in nitrification, NH$_3$ oxidation, involves the oxidation of NH$_3$ to the intermediate hydroxylamine (NH$_2$OH) and eventually nitrite (NO$_2^-$). This process

is mediated by both ammonia-oxidizing archaea (AOA) in the phylum Thaumarchaeota (5) and ammonia-oxidizing bacteria (AOB), such as *Nitrosomonas* and *Nitrosococcus* (6). In many soils, AOA greatly outnumber AOB, which has led to the hypothesis that AOA abundances control nitrification rates in terrestrial ecosystems (7–9). This is presumed to be especially true in acidic forest soils, where AOA tend to dominate due to their unique metabolic adaptations (10–12). However, the degree to which AOA vs. AOB influence NO$_y$ emissions from soil is unknown (13) and may depend on the fate of NH$_2$OH. NH$_2$OH can decompose via abiotic or enzymatic pathways to nitrogen oxides and NO$_2^-$ (14). NO$_2^-$ can then be volatilized as HONO or oxidized to NO$_3^-$ via nitrite-oxidizing bacteria (NOB), such as *Nitrobacter* (15). NO$_2^-$ can also sequentially convert to NO, N$_2$O, and N$_2$ via nitrifier denitrification or denitrification (16). While many of these N-cycle pathways leading to NO and nitrous oxide (N$_2$O) production are fairly well described (17–19), investigations of the relationships between nitrification and NO$_y$ fluxes from field soils are rare.

Of the nitrogen oxides produced during nitrification, NO tends to receive less attention than the strong greenhouse gas, N$_2$O. However, after it is released by N-cycle microbes, NO can escape the soil and contribute indirectly to atmospheric radiative forcing through its influence on tropospheric ozone formation (1, 13); it also mediates the oxidizing capacity of the atmosphere via the cycling of HO$_x$ ($\equiv$ OH + HO$_2$) (20). It was recently hypothesized

Significance

Reactive nitrogen oxides (NO$_y$) can negatively impact air quality, visibility, and human health. Biogenic sources of NO$_y$ are poorly understood despite their growing importance in future scenarios of decreasing anthropogenic emissions. Using soil from two forest stands that differ in plant and soil characteristics, we show that ammonia-oxidizing bacteria and to a lesser extent, heterotrophic microbes are the primary producers of NO$_y$. Moreover, we show that ammonia-oxidizing archaea contribute little to NO$_y$ yet play a central role in determining nitrogen-cycle rates in forests. Given known relationships between tree species and soil characteristics, we conclude that NO$_y$ emissions are spatially variable, occurring in hotspots throughout the eastern United States.

Fig. 1. Overview of soil N-cycle processes showing major transformations and products. Color shading indicates process grouping: gray (nitrification), red (nitrifier denitrification), and blue (denitrification).

that AOA require NO as a coreactant during the dehydrogenation of NH_2OH, whereas AOB do not (21), implicating AOB as the predominant biological source of NO from soil. Furthermore, Caranto and Lancaster (22) showed that NO is a precursor to NO_2^- in AOB via the NH_2OH/NO obligate intermediate mechanism, indicating a possible biogenic pathway for aerobic-derived NO. Evidence for AOB contributing to NO release comes from culture-based assays showing that AOB produces significantly more NO than AOA (14, 21). However, this phenomenon has yet to be demonstrated in a soil matrix, leading to questions regarding the environmental significance of this proposed mechanism. Furthermore, AOA have been shown to produce N_2O via the spontaneous hybrid formation pathway involving the reaction of NO with NH_2OH (23). Thus, elucidating the primary source of NO emissions may help quantify the relative amount of N_2O produced by archaeal NH_3 oxidation. Recently, Taylor et al. (24) reported an assay for discriminating between AOA and AOB nitrification through the use of gaseous amendments that selectively bind to either AOB ammonia monooxygenase (AMO; i.e., 1-octyne) or both AOA and AOB AMO (acetylene), rendering the enzyme irreversibly inactive. While this assay has been used to discriminate sources of NO_2^-, NO_3^- (25), and N_2O (26, 27) production, it has not been used to partition the sources of nitrification-derived NO.

Another emerging question is the role of nitrifying microbes in the production of HONO, which is a major source of atmospheric OH and NO (28). Vertical gradients of HONO have been observed with the highest concentrations at ground level (29–32), indicating that HONO production may be a function of biotic and/or abiotic soil processes. Most studies have implicated abiotic mechanisms associated with NO_x (NO and NO_2) chemistry as the primary driver of HONO production. However, it has recently been suggested that a portion of the NH_2OH produced via NH_3 oxidation is released from the soil as HONO (14, 33), assuming that certain conditions associated with soil pH, water content, and surface area are met (34, 35). Additionally, biologically produced NO_2^- may be protonated to form HONO. A recent study by Scharko et al. (36) showed that HONO production could be decreased by the addition of nitrification inhibitors, indicating its association with nitrification. The authors used flux measurements and amplicon sequencing to determine links between the relative abundances of AOA, AOB, and NOB and HONO production; they noted that, in near-neutral pH soils, HONO flux was highest and AOB were most abundant, whereas in acidic soils, HONO was lower and AOA dominated, possibly indicating a pH-influenced source of biogenic HONO. Studies of pure cultures of AOA, AOB, and NOB indicate that lineages of AOA and AOB can potentially produce HONO; however, AOB seem to be the dominant contributors in laboratory cultures (14). The discovery by Caranto and Lancaster (22) that NO is a necessary intermediate of AOB nitrification may have direct implications on HONO production. Considering that the NH_2OH/NO obligate intermediate mechanism implicates NO as a direct precursor to NO_2^- (22), the relative amount of NO lost from the cell vs. the amount oxidized to NO_2^- will directly influence HONO emissions, especially if a large portion of the produced NO_2^- is released into an acidic soil matrix. Similar to NO flux, it is unclear which tax-

onomic group is the major contributor to HONO emissions under environmental conditions or if there are other biogenic sources of HONO, such as heterotrophic bacteria and fungi.

Forests are often presumed to be strong sources of NO_y (37, 38). However, determining the importance of these gases at an ecosystem or regional scale has been challenging owing to the high degree of inter- and intrasystem variability of many N-cycling processes (7, 39–41). Thus, there is a need to develop predictive frameworks that identify hotspots for reactive nitrogenous gas fluxes in forests dominated by different biotic communities and underlain by variable edaphic properties. Deciduous forests of the eastern and midwestern United States are generally composed of a mixture of tree species that associate with either arbuscular mycorrhizal (AM) fungi or ectomycorrhizal (ECM) fungi. This mycorrhizal differentiation has been shown to be an effective trait integrator leading to "biogeochemical syndromes" as summarized by the mycorrhizal-associated nutrient economy (MANE) hypothesis (42). In general, soils in stands dominated by ECM species have litter and soil pools that are rich in organic N with relatively large C:N ratios. AM soils are much richer in inorganic N, possess smaller C:N ratios, and have relatively high rates of net nitrification (43). Both stand types possess acidic soils (pH 3.5–5.5), although ECM soils tend to be more acidic than AM soils. Given that most forests contain a mixture of AM and ECM trees, "mycorrhizal gradients" (plots varying in their abundance of AM or ECM trees) represent ideal systems for quantifying sources and mechanisms of nitrogen oxide production.

In this study, we investigate which factors control aerobic NO_y production in deciduous forest soils of the midwestern United States and advance a predictive framework for estimating these fluxes at ecosystem and regional scales. We hypothesize that NO_y fluxes are a function of ammonium oxidizer abundances (especially AOB, which are presumed to be the primary source of aerobic NO_y production), soil pH, and the abundance of AM-associated tree—all factors that have been linked previously to high nitrification rates (42, 44) and can be used to predict fluxes in field soils.

Results and Discussion

AOA Mediate Net Nitrification Rates in AM Soils but Not in ECM Soils.
We observed large differences in net nitrification between AM and ECM soils and in response to inhibitor additions (Fig. 2). Overall, net nitrification rates in AM soil were roughly 10 times higher than rates in ECM soils, which were generally below detection. Greater nitrification rates in AM soils relative to ECM soils have been observed previously (42, 43), although the underlying factors responsible for this pattern remained elusive. Inhibitor experiments suggest that AOA are primarily responsible for nitrification in AM soils. However, AOB do contribute to NO_2^- + NO_3^- accumulation—albeit to a lesser extent. The addition of 1-octyne (which inhibits AOB) had limited effects on nitrification in AM soils, resulting in a decrease of 0.13 µg N per gram of soil per day. However, the addition of acetylene (which inhibits AOA and AOB) decreased nitrification (relative to the 1-octyne treatment) by 0.47 µg N per gram of soil per day, indicating that the AOA populations contribute to nitrification to a greater extent than AOB. In contrast, inhibition of AOA and AOB had no effect on nitrification in ECM soils.

qPCR was used to quantify the abundance of bacterial and archaeal NH_3 oxidizers [via ammonia monooxygenase subunit A (amoA)] in soils. We found that, while AOA were more abundant than AOB for a given soil type, there were no differences in the AOA population between AM and ECM soils (Fig. 3). AOA abundance explained a significant amount of variability in net nitrification rates (58%) in AM soil but not in ECM soil (*SI Appendix*, Fig. S1), indicating that their comparable presence in ECM soil was not indicative of NO_2^- + NO_3^- accumulation. Moreover, the addition of acetylene had no significant effects on net nitrification in the ECM soils, indicating that inhibition of
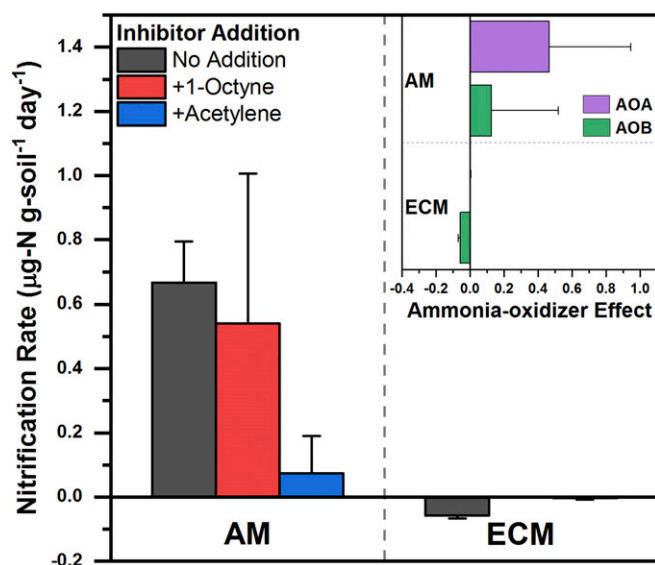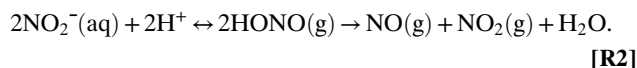
Fig. 2. Rates of total, 1-octyne, and acetylene net nitrification. *Inset* indicates the NH_3-oxidizer effect on nitrification rates for AM and ECM soil, which for AOB, is calculated as the difference in nitrification rate between the no inhibitor and 1-octyne treatments. For AOA, NH_3-oxidizer effect is calculated as the differences between nitrification rate under 1-octyne and acetylene additions ($n = 8$).

AOA did not change the net production of $NO_2^- + NO_3^-$. Given that net nitrification rates were generally below detection limits, an important question is why ECM soils have such low rates, although AOA abundance was similar to AM soil. One hypothesis is that the low pH of ECM soils limits nitrification. In a previous study conducted at the same research site as this study, Vitousek and Matson (45) showed that the addition of a liming agent (Na_2CO_3) increased NO_3^- production in ECM soils. However, when we repeated this experiment with our soils, we were unable to significantly increase nitrification rates, even when soil pH was raised from 3.5 to 7 and soil was fertilized with an ammonium supplement (*SI Appendix*, Fig. S2). Whether the low nitrification rate in ECM soils results from greater microbial assimilation of NO_3^-, thereby preventing net NO_3^- accumulation (46), or some other mechanism [e.g., chemical inhibition via volatile organic compounds (47, 48)] warrants additional study.

Despite Lower Abundances than AOA, AOB Control NO_y Soil Outgassing. NO_y fluxes between AM and ECM soil were quite divergent, with AM soil producing significantly greater flux of NO, NO_2, and HONO relative to ECM soil (Fig. 4). Furthermore, the difference in NO_y production when select NH_3 oxidizers are inhibited (defined as the NH_3-oxidizer effect) (described in *Methodology*) shows that AOB were the primary drivers of NO_y production, which is contrary to what was shown for nitrification rates. This suggests that there is some physiological mechanism by which AOB are more prone to lose nitrification substrates via volatilization relative to AOA. This could primarily be a function of NH_2OH loss and subsequent conversion to NO_y by abiotic processes in soil. Specifically, both AOA and AOB have the potential to release NH_2OH to the extracellular matrix during NH_3 oxidation (14). However, some AOA taxa have been shown to release far less relative to AOB (49). This may be a result of the uncharacterized NH_2OH-oxidizing enzyme in AOA, which may have a higher affinity for NH_2OH relative to the functionally similar one found in AOB. Thus, it is likely that NO_y outgassing under aerobic soil conditions are initiated by AOB enzymatic activity.

Interestingly, not all NO_y gas fluxes behaved identically, indicating possible differentiation in production mechanisms (Fig. 4).

NO flux values were similar to another incubation-based experiment using deciduous forest soil from the eastern United States (19). In regard to inhibitor addition, AM soil NO flux decreased by one-half when 1-octyne was applied, which was equivalent to NO flux when acetylene was added. This indicates that, in AM soil, AOB contribute roughly one-half of the NO produced, and the other one-half can be attributed to abiotic or heterotrophic sources. The observation that AOA did not contribute to NO production is consistent with the NO intermediate mechanism postulated by Kozlowski et al. (21) and pure culture observations by Ermel et al. (14). The primary mechanism for NO production is likely a combined effect of NH_2OH released into the extracellular matrix (49) and subsequent abiotic processes, the biological-derived release of NO by AOB during NH_2OH oxidation, and NO_2^- reduction during nitrifier denitrification (22, 50). Any NO produced by AOA is not released from the cell and rather, is utilized during NH_2OH dehydrogenation (21). NO fluxes in ECM soil were generally low and did not change in response to inhibitors, indicating heterotrophic or abiotic sources. Considering the lack of net $NO_2^- + NO_3^-$ production in the presence of acetylene, an abiotic mechanism is the most likely NO source in ECM soils. As shown in a supplementary experiment (*SI Appendix*, Fig. S3), where AM and ECM soils were individually coated on the walls of flow tubes and subjected to HONO, both soils are capable of abiotically converting HONO into NO, most likely through reaction **R1** where gaseous HONO is deposited on the soil surface as NO_2^- and subsequently reacts with iron oxides in the process of chemodenitrification (16, 35, 51). Alternatively, as shown in reaction **R2**, NO may also be formed in acidic soil through the self-decomposition of NO_2^- via HONO (52). However, due to second-order dependence on HONO concentration, **R2** is predicted to be more important at higher concentrations of HONO. Under environmentally relevant levels of HONO, **R1** is likely the more important pathway for abiotic NO formation:

$$NO_2^-(aq) + Fe^{2+} + 2H^+ \rightarrow NO(g) + Fe^{3+} + H_2O \qquad \text{[R1]}$$

$$2NO_2^-(aq) + 2H^+ \leftrightarrow 2HONO(g) \rightarrow NO(g) + NO_2(g) + H_2O. \qquad \text{[R2]}$$

Decomposition of NO_2^- to NO is facilitated at low pH (53), consistent with the supplementary experiment showing that, when HONO is flowed over both AM and ECM soils, higher NO
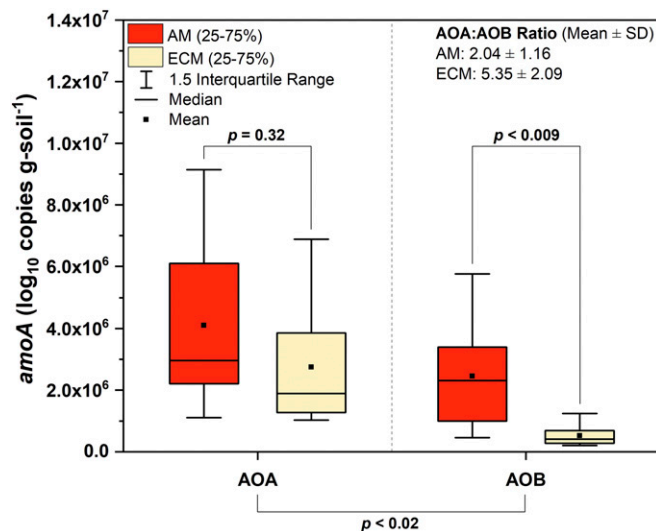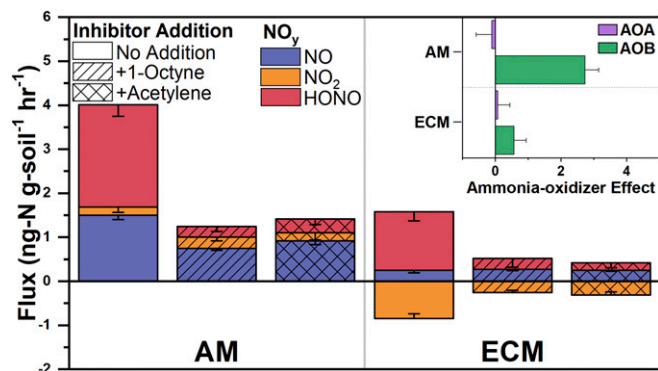

Fig. 3. Quantification of AOB and AOA *amoA* based on copy number per gram of soil ($n = 8$). *Inset* indicates the ratio of AOA to AOB.

Fig. 4. Mean fluxes of NO, NO_2, and HONO from hours 14, 15, and 16 of their respective incubation in response to inhibitor additions ($n = 8$). *Inset* indicates the NH_3-oxidizer effect on NO_y fluxes, where the AOB effect is the difference in nitrification rate between the no inhibitor and 1-octyne treatments and the AOA effect is the difference between nitrification rate under 1-octyne and acetylene additions. NH_3-oxidizer effect is based on the combined effect of all NO_y gases (NO, NO_2, and HONO).

flux is observed from the more acidic ECM soil. Considering the decline of NO flux with decreasing water content in ECM soil, there is also the possibility that denitrification-derived NO is being produced in anaerobic microsites, which have more access to O_2 as the soil dries out. Alternatively, it could be that the lack of $NO_2^- + NO_3^-$ accumulation in ECM soil is related to higher NO_2^- to NO conversion via nitrifier denitrification, which would prevent accumulation of NO_2^- and allow AOA to utilize the produced NO; unfortunately, this cannot be verified, because quantification of NO_2^- was made simultaneously to NO_3^-. Another interesting consequence of the high flux of NO in AM soils is the potential for higher N_2O production via the spontaneous hybrid pathway (23). On average, N_2O flux was negative and decreased only when AOB were inhibited (*SI Appendix*, Fig. S4), indicating that the majority of N_2O being produced was from AOB-derived nitrifier denitrification and was not from AOA via spontaneous hybrid formation. The overall negative flux (or sink) of N_2O may be a function of the disproportionally large diversity of organisms able to reduce N_2O to N_2 without first producing N_2O relative to the low abundance of N_2O-producing taxa, such as AOB (54).

AM soils produced positive flux for NO_2, which did not change with inhibitor additions, while ECM soil produced negative fluxes that became more positive with the addition of inhibitors; however, it is unclear what led to this observation. In the atmosphere, NO_2 can stem from the reaction of ozone with NO after it is emitted from soil. Our observations are not affected by this reaction, since ozone was not present in the zero air used for our laboratory chamber experiments. Rather, our evidence suggests that the NO_2 emitted from AM soil is of biological origin and that it is likely formed from the reaction of other nitrification intermediates (e.g., the reaction of NO and O_2 on soil surfaces as well as NH_2OH decomposition) (55, 56). Previous studies also suggest NO_2 emitted from soil to be of biological origin, perhaps a product of heterotrophic processes. For example, it was found that NO_2 amounted to as much as 10% of the NO_x flux measured (57–59) from agricultural plots. However, it should be kept in mind that chemiluminescence instruments used in earlier studies measured NO_2 using Mo-converter channels, which indiscriminately converted other forms of NO_y to NO; this biases the measurement in favor of higher NO_2 concentrations (59). Our method of detecting NO_2 is not prone to such artifacts, since we photolyze NO_2 at a wavelength (395 nm) not absorbed by most NO_y species and we correct for the amount of HONO that does absorb at this wavelength (60).

Consistent with the other two NO_y gases, HONO production was significantly higher in AM soil. HONO flux was reduced significantly when 1-octyne was added, indicating that the main source is AOB nitrification. The likely mechanisms for the production of HONO are enzymatic and abiotic oxidation of NH_2OH (14, 33) with subsequent protonation of NO_2^- in the soil matrix. Higher HONO production in AM soils is directly related to higher levels of net nitrification. The fact that HONO is linked to AOB activity lends to the idea that AOB are actively nitrifying, although they are in the minority relative to AOA. Additionally, this may indicate that AOA and AOB have a relatively equivalent rate of NH_3 oxidation. However, because of loss pathways, AOB do not contribute greatly to net nitrification rates. We suggest that higher AOB contribution to HONO production is primarily a function of abiotic synthesis from extracellular NH_2OH. It should also be mentioned that a fraction of the HONO flux for all treatments could be a result of NO_2 to HONO conversion through iron (61) and soil organic matter-mediated chemistry (62). This is especially true for unamended ECM soil, where deposition of background NO_2 was accompanied by a positive flux of HONO.

On the Mechanisms Responsible for Fluxes of NO_y from Forest Soil. The inhibitor experiments show that AOB are primarily responsible for NO_y fluxes while AOA are primarily responsible for $NO_2^- + NO_3^-$ production; however, AOB are also nitrifying. As noted above, a possible reason for AOB dominance in NO_y production is due to the high affinity of AOA for nitrification-derived substrates, such as NH_2OH. We summarize a potential mechanism for aerobic nitrogen oxide production in Fig. 5. In short, both AOB and AOA oxidize NH_3 to NH_2OH. However, some of the NH_2OH produced by AOB is lost from the cell due to lower affinity for NH_2OH, whereupon it is decomposed abiotically to various nitrogenous gases. This initial step in nitrification occurs more frequently for AOB in moderate pH soils, leading to high NO_y fluxes in AM soil relative to ECM soils. NH_2OH produced in the initial step can be directly oxidized by AOA to NO_2^-. However, AOB have been shown to produce NO as an intermediate via the NH_2OH/NO obligate intermediate mechanism, whereas AOA do not (22). In theory, AOB can release this NO from the cell, whereupon it can be utilized by AOA to dehydrogenate NH_2OH, possibly indicating a pseudosymbiotic relationship between AOA and AOB under aerobic conditions. Because of their more conservative approach to nitrification intermediates (49), AOA are shown here to be the primary contributors to $NO_2^- + NO_3^-$ production under aerobic
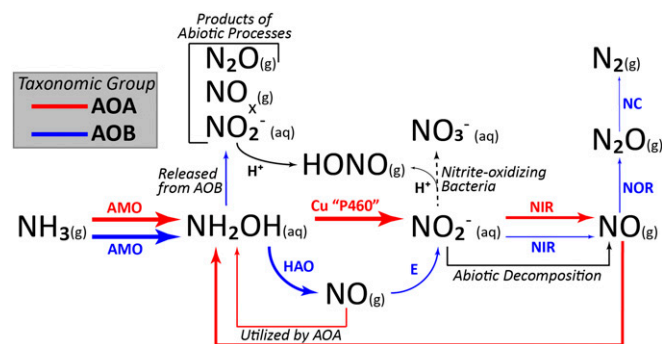
**Fig. 5.** Proposed mechanism for AOA- and AOB-dependent NO_y production. Arrow width symbolizes the amount of substrate being transformed relative to starting substrate (i.e., NH_3). Enzymes are listed above arrows. Cu "P460," putative copper-containing enzyme; E, unknown nitric oxide oxidoreductase; HAO, hydroxylamine oxidoreductase; NC, nitrosocyanin; NIR, nitrite reductase; NOR, nitric oxide reductase.

conditions, whereas AOB contribute less to the nitrification rate due to some of the initial NH_3 being lost from the cell as NH_2OH and NO. It is also possible that some of the produced NO_2^- is lost during the transfer from AOA and AOB to NOB and subsequently protonated to HONO or reduced to NO (52). Such loss of NO_2^- during transfer has been shown to be prevalent in drying soils (53). Considering that both NO and HONO fluxes decreased when AOB were inhibited, it is possible that NH_2OH oxidation-derived NO is directly related to HONO production, most likely through the production and subsequent protonation of NO_2^-. It is also conceivable that NO_2^- can be reduced to NO via the nitrifier denitrification pathway within anaerobic microsites. Following this step, NO can be reduced by AOB to N_2O and N_2, or AOA can recycle it during the dehydrogenation of NH_2OH. As noted previously, aerobic N_2O production is primarily attributed to AOB (*SI Appendix*, Fig. S4), indicating that it is not likely formed from the AOA-derived spontaneous hybrid mechanism in these soils.

Primary Controls of NO_y Production Can Be Used to Predict Flux. Using a stepwise linear regression, soil pH was found to be the best predictor of peak NO and NO_2 flux, while nitrification rate best predicted HONO flux (*SI Appendix*, Table S1). The observation that soil pH explained a significant amount of variation in NO flux is likely due to a concurrent relationship between AOB activity and flux. That is, we have shown that the predominant autotrophic source of NO flux from soil is AOB, which tend to be most abundant in less acidic environments, such as AM soil (Fig. 3). If the major factor in NO production is the activity of AOB via NH_2OH oxidation and nitrifier denitrification, then it is no surprise that the predicted fluxes are generally higher in AM-dominated forest soil relative to ECM soil. This is predominately due to the assumed limitations of AOB at more acidic pH as observed in ECM stands. Other studies have shown higher NO flux at low soil pH (<4.5), which has primarily been attributed to higher rates of chemodenitrification (63). Although the AM soil was more alkaline than the ECM soil, it was still quite acidic (soil pH 4.8 ± 0.2) and did possess excess nitrification products that were likely subjected to biotic and abiotic reduction. Considering that chemodenitrification-derived NO is more prevalent in acidic soil, not seeing large fluxes from ECM soil was surprising. We believe that this is a function of low rates of net nitrification, which will require additional investigation. We see the same relationship between NO_2 flux and soil pH with higher NO_2 flux in less acidic soil. This is to be expected if NO_2 stems from an abiotic reaction involving an NO precursor on soil surfaces. The relationship between HONO flux and nitrification rate is most likely a function of biogenic NH_2OH and NO_2^- serving as the precursor to HONO production.

A map of NO_y flux across the eastern United States was generated using the aforementioned NO_y relationships with soil pH and nitrification rates, which were extrapolated across the eastern United States using georeferenced plots of known AM and ECM tree abundance (Fig. 6). This figure illustrates that there are clear trends in NO_y production with putative hotspots occurring throughout several ecological provinces within the eastern United States, including the Central Interior Broadleaf Forest, the Eastern Broadleaf Forest, the Lower Mississippi Riverine Forest, and the Midwest Broadleaf Forest. The soils within each of these ecological provinces possess a generally moderate pH and narrow C:N, which likely correspond to higher NO_y flux via higher rates of NH_2OH and NO_2^- production. By averaging all predicted NO_y fluxes, we estimate that forest soils throughout the eastern United States produce 147 ± 68 µg NO_y-N per square meter per hour. Previous studies that have measured fluxes of NO_y focused on NO. Studies that report NO flux values from forests are highly skewed toward ECM forests (*SI Appendix*, Table S2), which makes comparisons difficult and il-
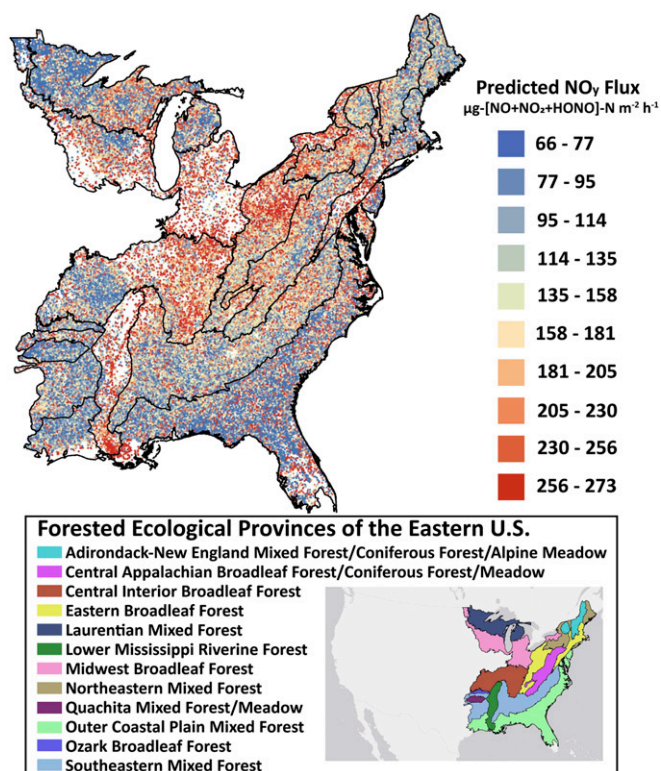
Fig. 6. Map of estimated NO_y flux based on mycorrhizal association for forest inventory analysis data points throughout the eastern United States. Areas are segmented into ecological provinces of the eastern United States.

lustrates the importance of our measurements. However, the few studies that investigate NO flux from AM and ECM soils are in agreement with our observation that AM soil produces more NO relative to ECM soil (64, 65). Of our estimated average value for NO_y, 37% is attributed to NO, which corresponds to 52 ± 17 µg NO-N per square meter per hour. This value is slightly higher than most field-based measurements of NO (*SI Appendix*, Table S2), which is likely a result of our estimates being based on peak values at optimum soil water conditions. In that regard, our values may represent the upper bounds of NO_y emissions from forest soil. One drawback of our analysis is the lack of coniferous forest data. As shown in *SI Appendix*, Table S2, some coniferous ECM soils have been shown to surpass deciduous AM soils in NO flux. Subsequent NO_y measurements, calculations, and extrapolations based on the MANE framework will need to take into account independent tree species abundance in addition to mycorrhizal status.

Although our NO_y flux measurements did not consider all NO_y species (i.e., N_2O_5, peroxyacyl nitrates, and alkyl nitrates) and were generated from laboratory incubations from a single site and season, our estimates provide a direct linkage between NO_y fluxes and overstory forest composition, microbial communities, and edaphic characteristics. Such relationships are critical for scaling estimates over large geographic regions. Nevertheless, an important next step is to verify our estimates using soils collected from other sites and seasons, which will yield insights on how NO_y emissions from AM and ECM soils vary spatially and temporally (e.g., across different soil mineralogy and in response to fluctuations in soil moisture, temperature, and substrate availability). Additionally, the degree to which N deposition affects regional NO_y fluxes is an open question. Although previous investigations indicate that N deposition effects on NO_y emissions may hinge on the type of forest cover and

ENVIRONMENTAL SCIENCES

other soil characteristics (66), spatial trends of NH_4^+ and NO_3^- deposition (67) coincide with midwestern hotspots that could have synergistic effects in promoting NO_y emissions from AM soils in these areas. Interestingly, our highest predicted NO_y flux value (273 μg N m^{-2} h^{-1} ~ 24 kg N ha^{-1} y^{-1}) coincides strongly with values associated with the highest N deposition values observed in the midwestern United States (>20 kg N ha^{-1} y^{-1}) (67). Furthermore, the high levels of N deposition in these areas may be promoting the establishment of AM trees in previously ECM-dominated areas, which would indirectly promote higher rates of NO_y emission from soil (68). Continued work on estimating NO_y flux will inevitably need to take into account other environmental factors, including climate effects.

Conclusions

We presented evidence that identifies AOA as the predominant NH_3-oxidizing taxa in AM- and ECM-dominated forests stands. In contrast, AOB are the predominant autotrophic source of nitrification-derived NO_y from soil. We attribute this lack of AOA-derived flux to their metabolic utilization of NO as a nitrification intermediate, high affinity for NH_2OH, and lack of producing NO as an intermediate during NH_2OH oxidation. There is also evidence to suggest abiotic and heterotrophic mechanisms contribute to nitrogen oxide flux, although additional studies will be necessary to pinpoint exact taxa and/or mechanisms responsible for this flux. Our results also contribute to the ever-growing characterization of differences between AM- and ECM-dominated stands by showing that AM soils produce significantly more NO_y than ECM soils. This coincides strongly with the already reported higher rates of net nitrification, narrower C:N ratios, and less acidic soil pH. We do not believe that the mycorrhizal symbionts are directly involved in the flux of NO_y, but considering that they do compete for mineral N, there is potential for indirect competition with nitrifying microbes. Finally, soil pH and nitrification rates were found to best explain NO_y fluxes, enabling us to utilize these relationships to predict NO_y flux throughout the eastern United States based on percentage ECM tree abundance. Using this framework, we estimate that hotspots may be found throughout broadleaf forests of the Midwest and the eastern United States as well as the Mississippi River corridor. Parameterizations based on widely available data hold promise for improving the accuracy of land surface models in representing soil NO_y emissions to the atmosphere; however, they will need to be validated before widespread implementation.

It is particularly important to accurately represent soil NO_y emissions in models that include regions covered in hardwood forests. Not only is land use change prevalent in these regions, but high emissions of biogenic volatile organic compounds (BVOCs), such as isoprene, lead to high BVOC/NO_x ratios. This combined with the fact that troposphere ozone concentrations have decreased in the United States by 30–40% over the past decade due to vehicle and point source emission reductions (69) means that ozone formation in many regions of the eastern United States will be particularly sensitive to small changes in NO_x. In such NO_x-limited regions, soil emissions could be major drivers of regional atmospheric chemistry.

Methodology

Study Area and Soil Sampling. Soil was sampled in August 2017 from a well-characterized nitrification gradient at Moores Creek Research and Teaching Preserve (39°05′ N, 86°28′ W) (43). This area is dominated by fine loamy, mixed, semiactive, mesic Typic Hapludults in the Brownstown–Gilwood series. Soil from four AM- and ECM-dominated stands (dominance implies >85% of the basal area of the stand) was sampled to a depth of 15 cm and separated by horizon (O = 0–5 cm; A = 5–15 cm). Each stand represented two 20 × 20-m² paired plots, where one plot was treated with $(NH_4)_2SO_4$ and $NaNO_3$ granular fertilizer monthly (May to October) since May 2011, resulting in 50 kg N ha^{-1} y^{-1}. For each monthly fertilizer application, the mass ratio of ammonium to NO_3^- was equivalent. In each plot, five soil cores

were sampled and separated by depth, and then, each depth increment was pooled to increase mass and reduce environmental heterogeneity [n = (4 pooled soil samples for each mycorrhizal type) × (2 fertilizer treatments) × (2 soil depths)]. Additionally, a separate soil core was taken for bulk density calculations in each plot. All samples were transferred on ice packs to the laboratory, where they were aseptically homogenized by hand, and an ~20-g subsample was immediately stored at −80 °C for future nucleic acid extraction. The remaining soil was stored at 4 °C until processing and subsequent analyses. Given that no fertilizer effects were apparent in the nitrification, qPCR, or gas flux assays, fertilized and unfertilized samples were pooled for statistical analysis (n = 8). Additionally, although the 5- to 15-cm depth increment was significantly different from the 0- to 5-cm increment, for multiple variables, it did not lead to noteworthy stand-type differences, and therefore, all analyses noted in *Results and Discussion* are for 0–5 cm.

Soil Physicochemical Analyses. Soil pH was determined by using an Orion pH meter (ThermoFisher Scientific) on a 1:2 solution of air-dried soil in a 0.01 M $CaCl_2$ solution. An intact field-moist soil core for each depth (0–5 and 5–15 cm) was used to calculate bulk density using Eq. **1**,

$$BD = \frac{[m_{soil} - (m_{soil} \times GWC)]}{V},$$ [1]

where BD is bulk density in grams soil centimeter^{-3}, m_{soil} is the total mass of the soil core, GWC is gravimetric water content calculated as the mass of water in the soil sample divided by the dry mass of soil, and V is the volume of the soil core. The pooled samples were passed through a 2-mm sieve to homogenize the soil and remove large organic fragments, roots, and rocks. A 10-g aliquot of sieved soil was then dried at 60 °C for 48 h and finely ground into powder using a mortar and pestle. The pulverized soil was used to determine the concentration of total soil carbon and total soil N using a Costech ECS 4010 elemental analyzer (Costech Analytical Technologies Inc.). Environmental levels of NH_4^+ and $NO_2^- + NO_3^-$ were quantified from 4 g of sieved field-moist soil with 15 mL of 2 M KCl within 36 h of soil being taken from the ground and analyzed using a Lachat QuikChem 8000 Flow Injection Analyzer (Lachat Instruments). The method for measuring NO_2^- and NO_3^- was based on cadmium reduction, where NO_3^- in the KCl extract is reduced to NO_2^- and the concentration is reported as $NO_2^- + NO_3^-$. Soil properties are summarized in SI Appendix, Table S3.

Quantification of amoA Gene Copy Number. Nucleic acids were extracted from 0.3 to 0.4 g field-moist soil using a DNeasy PowerSoil Kit (Qiagen). To obtain a field estimate of NH_3-oxidizer community size, the abundances of AOA and AOB were assessed by qPCR of the amoA gene using the same primers and protocol noted in Mushinski et al. (25) on a QuantStudio 7 Flex Real-Time PCR System (ThermoFisher Scientific). Amplification efficiencies of 72–83% and 76–86% were observed for AOA and AOB, respectively, with r^2 values >0.95. It should also be mentioned that the primer sets used in this study do not survey an NO_2^--oxidizing bacterial genus *Nitrospira*, which has recently been reported to also oxidize NH_3 (70). The addition of this taxa into the AOB grouping may lead to an alteration in the AOA:AOB ratio.

Nitrification Rates. Total nitrification rates in the presence and absence of 1-octyne or acetylene were determined using the AOA/AOB inhibition method described by Taylor et al. (24) for all samples. Specifically, 10 g of field-moist soil was weighed out in quadruplicate into 125-mL Wheaton bottles. The bottle openings were covered with parafilm, and the parafilm was punctured five times to allow for gas exchange. The parafilm was then covered with a wetted paper towel to maintain soil water content within the bottle and wrapped in aluminum foil. Soils were then preincubated in the dark for ~48 h at ambient room temperature (~23 °C). After preincubation, one analytical replicate was used to calculate background NH_4^+ and $NO_2^- + NO_3^-$ levels by immediately extracting soil inorganic N with 25 mL of 2 M KCl. The remaining three analytical replicates were capped and sealed with butyl stoppers. The second analytical replicate was used to calculate total nitrification and left unamended. The third analytical replicate was treated with acetylene (6 μmol L^{-1}) to completely block autotrophic nitrification. Acetylene was prepared by making a 10-fold dilution into 125 (vol/vol) mL of air and then adding 300-μL aliquots of the mixture to the 125-mL Wheaton bottle containing soil. The fourth analytical replicate was treated with 1-octyne (4 μmol L^{-1}) to selectively inhibit bacterial AMO. This AOB inhibitor was prepared by adding several glass beads to an empty 125-mL Wheaton bottle fitted with a butyl stopper. Liquid 1-octyne (40 μL) was then added to the bottle and overpressurized with 100 mL of air. The bottle was shaken vigorously for 1 min, and 2.7 mL of 1-octyne gas was added to the fourth replicate. The three analytical replicates were incubated at room temperature for 48 h followed by

soil inorganic N extraction with 25 mL of 2 M KCl. Extracts were analyzed for NH_4^+ and $NO_2^- + NO_3^-$ as noted above. Total net nitrification rates were based on the accumulation of $NO_2^- + NO_3^-$ in the absence of gaseous inhibitors and attributed to all potential sources (i.e., AOB, AOA, and heterotrophic microbes). Net nitrification in the presence of 1-octyne was attributed to AOA and heterotrophic microbes, while in the presence of acetylene, nitrification was attributed solely to heterotrophic microbes. Rates of ammonification are shown in SI Appendix, Fig. S5. Rates of mineral soil nitrification mimic the trends shown in 0–5 cm (Fig. 2) but are, on average, 50–80% lower.

Quantification of Soil Gas Fluxes. Fluxes of CO_2, N_2O, NO, NO_2, and HONO were measured from soil using a continuous flow soil incubation system coupled to a chemiluminescent NOx + HONO analyzer (Air Quality Design, Inc.) and a cavity ringdown infrared N_2O analyzer (Los Gatos Research, Inc.). A detailed description of the analytical systems can be found in SI Appendix, Fig. S6. Three analytical aliquots per sample (30 g) were sealed in airtight 125-mL Wheaton bottles capped with a butyl stopper. The first replicate was normalized to 40% GWC by adding sufficient ultrapure water to soil and was subsequently used to quantify total flux from soil. By the end of the experiment, all soils had reached 0% GWC. Fluxes of CO_2, N_2O, NO, and HONO were measured from soil over the subsequent 48-h period and calculated according to Eq. 2:

$$Flux_i = \frac{1}{\tau} \times \frac{F_{tot}\left(C_{i,soil} - C_{i,blank}\right)}{m_{soil}}. \qquad [2]$$

In Eq. 2, τ is the residence time of gas in the chamber, F_{tot} is the flow of the carrier gas through the chamber, m_{soil} is the mass of soil, and $C_{i,soil}$ and $C_{i,blank}$ are the concentrations of analyte gas i (i = NO, NO_2, HONO) measured within the soil containing and blank chambers, respectively. By the end of the incubation, soil had achieved 0% water content. It follows from Eq. 2 that positive fluxes describe net transfer of gases from soil to air, while negative fluxes represent net transfer from air to soil (i.e., deposition or consumption).

To inhibit AOB activity, 1-octyne (4 μmol L^{-1}) was added to the headspace of the second replicate and thoroughly shaken for 5 min followed by a 1-h rest period to allow for equal diffusion of 1-octyne throughout the soil. The soil GWC was then normalized to 40% by adding sufficient ultrapure water to the sealed Wheaton bottle via syringe. Additionally, the antibiotic kanamycin (final concentration in soil: 220 μg g^{-1} soil) was added to the soil during the water content normalization step to inhibit further bacterial synthesis of AMO (71). Soil was then allowed to preincubate for 24 h at room temperature. After preincubation, caps were removed from the Wheaton bottles, and soils were transferred to sterile 100-mm petri dishes and inserted into the sampling chamber. A third treatment was designed to inhibit all autotrophic nitrification. In this case, acetylene (6 μmol L^{-1}) was added along with the following compounds during the water normalization step: (i) the antibiotic kanamycin (220 μg g^{-1} soil) to inhibit any further synthesis of bacterial AMO, (ii) the archaeal protein synthesis inhibitor fusidic acid (800 μg g^{-1} soil), and (iii) the well-known nitrification inhibitor nitrapyrin (200 μg g^{-1} soil) to subdue any subsequent autotrophic nitrification. Flux values for all NO_y species from 48-h experiments are shown in SI Appendix, Figs. S7–S11. All values reported in Results and Discussion are means from 14, 15, and 16 h of each respective incubation. Fluxes for all N gases (i.e., N_2O, NO, NO_2, and HONO) are in nanograms N gram soil^{-1} hour^{-1}. Results from a mixed model ANOVA, where gas flux is defined as the dependent variable, are listed in SI Appendix, Table S4. Combined gaseous N balance for AM and ECM soils at 5–15 cm generally mimicked what was shown at 0–5 cm but was 40–60% lower. To test the capacity for AM and ECM soil to abiotically produce NO from the reactive conversion of HONO on soil surfaces, we utilized a jacketed horizontal flow tube equipped with a movable injector (34, 35) and attached to the chemiluminescence detector. A detailed description of this procedure is provided in SI Appendix, SI Materials and Methods.

Predicting Gas Fluxes Throughout Forests of the Midwest (United States). Mean NO_y (NO, NO_2, and HONO) flux (P_i) in nanograms N gram soil^{-1} hour^{-1} was subsequently converted to micrograms N per square meter per hour using Eq. 3,

$$P_i = Flux_i \times SBD \times d \times 10, \qquad [3]$$

where $Flux_i$ is gas flux of nitrogen oxide gas i (nanograms N gram soil^{-1} hour^{-1}), SBD is soil bulk density (estimated at 1.0 g soil cm^{-3}), and d is soil depth interval in centimeters (5 for the 0- to 5-cm increment or 10 for the 5- to 15-cm increment). Using P_i in a stepwise linear regression, we determined which factors are best suited at predicting peak nitrogen oxide flux. AM- and ECM-derived peak flux values for NO, NO_2, and HONO (0–5 cm) were used as response variables, while properties associated with three distinct categories [microbial community structure (AOA:AOB), background edaphic properties (soil pH, soil C:N, background NH_4^+), and process rates (net nitrification rate)] were used as independent variables. Models were selected based on the lowest Bayesian information criterion. Soil pH and net nitrification rate were found to be the best predictors of gas flux (SI Appendix, Table S1). We then compiled soil pH and nitrification rate data from eight AM and ECM sites throughout the Midwest, the eastern United States, and the southeastern United States. Specifically, four sites were in Indiana (Griffy Woods, Lilly Dickey State Forest, Moores Creek Research Area, and Morgan Monroe State Forest), one was in Missouri (Tyson Research Center), one was in Georgia (Whitehall Forest), one in Wisconsin (Wabikon Forest), and one was in North Carolina (Duke Forest). These data were then incorporated into the three NO_y-specific linear regressions (NO, NO_2, and HONO) compiled from the stepwise linear regression. We then regressed the predicted NO_y values against percentage ECM basal cover (SI Appendix, Fig. S12), which explained a significant amount of variation in predicted NO_y. The predicted equation output for NO_y in response to percentage ECM was applied to percentage ECM data compiled from over 78,000 forest inventory plots. NO, NO_2, and HONO values were summed to obtain an estimate of NO_y and then plotted onto a georeferenced map (ArcMap 10.3; Environmental Systems Research Institute) to obtain an estimate of NO_y flux hotspots.

Statistical Analyses. Statistical analyses and graphic visualization were performed using JMP Pro-13 (SAS Institute, Inc.), OriginPro (OriginLab, Inc.), and R (R Development Core Team). All datasets were tested for normality using Shapiro–Wilk's test. When data were not of normal distribution, $\log_{10}$ transformations were applied. For gas fluxes, the mean fluxes at 14, 15, and 16 h were used as normalized values for each biological replicate and analyzed accordingly. Soil biological, physicochemical, and flux data were statistically analyzed using a linear mixed model ANOVA where mycorrhizal type, fertilizer treatment, soil depth, and their interactions were fixed effects, plot replicate was designated as a random variable and nested within mycorrhizal type, and soil depth was designated as a repeated measure. Significant differences were inferred when $P < 0.05$. When differences were significant, Tukey's honest significant differences test was performed to assess post hoc contrasts. The NH_3-oxidizer effect was calculated for net nitrification rate and NO_y gas flux. For AOB, this represents the differences in net nitrification rate or NO_y flux between the no inhibitor and 1-octyne treatments, while for AOA, this was the difference between 1-octyne and acetylene additions.

1. Romer PS, et al. (2018) Effects of temperature-dependent NOx emissions on continental ozone production. *Atmos Chem Phys* 18:2601–2614.
2. Bouwman AF, Boumans LJM, Batjes NH (2002) Emissions of N2O and NO from fertilized fields: Summary of available measurement data. *Global Biogeochem Cycles* 16:6-1–6-13.
3. Kesik M, et al. (2005) Inventories of N2O and NO emissions from European forest soils. *Biogeosciences* 2:353–375.
4. Robertson GP, Groffman PM (2015) Nitrogen transformations. *Soil Microbiology, Ecology and Biochemistry*, ed Paul EA (Academic, Burlington, MA), 4th Ed, pp 421–446.

5. Stieglmeier M, et al. (2014) *Nitrososphaera viennensis* gen. nov., sp. nov., an aerobic and mesophilic, ammonia-oxidizing archaeon from soil and a member of the archaeal phylum Thaumarchaeota. *Int J Syst Evol Microbiol* 64:2738–2752.
6. Koops H-P, Pommerening-Röser A (2015) The lithoautotrophic ammonia-oxidizing bacteria. *Bergey's Manual of Systematics of Archaea and Bacteria*, eds Whitman WB, et al. (John Wiley & Sons, Inc., Indianapolis).
7. Prosser JI, Nicol GW (2008) Relative contributions of archaea and bacteria to aerobic ammonia oxidation in the environment. *Environ Microbiol* 10:2931–2941.

8. Prosser JI, Nicol GW (2012) Archaeal and bacterial ammonia-oxidisers in soil: The quest for niche specialisation and differentiation. *Trends Microbiol* 20:523–531.

9. Shen JP, Zhang LM, Di HJ, He JZ (2012) A review of ammonia-oxidizing bacteria and archaea in Chinese soils. *Front Microbiol* 3:296.

10. Lehtovirta-Morley LE, Stoecker K, Vilcinskas A, Prosser JI, Nicol GW (2011) Cultivation of an obligate acidophilic ammonia oxidizer from a nitrifying acid soil. *Proc Natl Acad Sci USA* 108:15892–15897.

11. Lehtovirta-Morley LE, et al. (2014) Characterisation of terrestrial acidophilic archaeal ammonia oxidisers and their inhibition and stimulation by organic compounds. *FEMS Microbiol Ecol* 89:542–552.

12. Lehtovirta-Morley LE, et al. (2016) Identifying potential mechanisms enabling acidophily in the ammonia-oxidizing archaeon "Candidatus *Nitrosotalea devanaterra*." *Appl Environ Microbiol* 82:2608–2619.

13. Conrad R (1996) *Metabolism of Nitric Oxide in Soil and Soil Microorganisms and Regulation of Flux into the Atmosphere* (Springer, Berlin), pp 167–203.

14. Ermel M, et al. (2018) Hydroxylamine released by nitrifying microorganisms is a precursor for HONO emission from drying soils. *Sci Rep* 8:1877.

15. Abeliovich A (2006) The nitrite-oxidizing bacteria. *The Prokaryotes*, eds Dworkin M, Falkow S, Rosenberg E, Schleifer K-H, Stackebrandt E (Springer, New York), pp 861–872.

16. Pilegaard K (2013) Processes regulating nitric oxide emissions from soils. *Philos Trans R Soc Lond B Biol Sci* 368:20130126.

17. Venterea RT, Rolston DE (2000) Mechanistic modeling of nitrite accumulation and nitrogen oxide gas emissions during nitrification. *J Environ Qual* 29:1741–1751.

18. Krämer M, Conrad R (1991) Influence of oxygen on production and consumption of nitric oxide in soil. *Biol Fertil Soils* 11:38–42.

19. Venterea RT, et al. (2003) Nitrogen oxide gas emissions from temperate forest soils receiving long-term nitrogen inputs. *Glob Change Biol* 9:346–357.

20. Steinkamp J, Ganzeveld LN, Wilcke W, Lawrence MG (2009) Influence of modelled soil biogenic NO emissions on related trace gases and the atmospheric oxidizing efficiency. *Atmos Chem Phys* 9:2663–2677.

21. Kozlowski JA, Stieglmeier M, Schleper C, Klotz MG, Stein LY (2016) Pathways and key intermediates required for obligate aerobic ammonia-dependent chemolithotrophy in bacteria and Thaumarchaeota. *ISME J* 10:1836–1845.

22. Caranto JD, Lancaster KM (2017) Nitric oxide is an obligate bacterial nitrification intermediate produced by hydroxylamine oxidoreductase. *Proc Natl Acad Sci USA* 114:8217–8222.

23. Stieglmeier M, et al. (2014) Aerobic nitrous oxide production through N-nitrosating hybrid formation in ammonia-oxidizing archaea. *ISME J* 8:1135–1146.

24. Taylor AE, et al. (2013) Use of aliphatic n-alkynes to discriminate soil nitrification activities of ammonia-oxidizing thaumarchaea and bacteria. *Appl Environ Microbiol* 79:6544–6551.

25. Mushinski RM, Gentry TJ, Dorosky RJ, Boutton TW (2017) Forest harvest intensity and soil depth alter inorganic nitrogen pool sizes and ammonia oxidizer community composition. *Soil Biol Biochem* 112:216–227.

26. Giguere AT, Taylor AE, Suwa Y, Myrold DD, Bottomley PJ (2017) Uncoupling of ammonia oxidation from nitrite oxidation: Impact upon nitrous oxide production in noncropped Oregon soils. *Soil Biol Biochem* 104:30–38.

27. Hink L, Gubry-Rangin C, Nicol GW, Prosser JI (2018) The consequences of niche and physiological differentiation of archaeal and bacterial ammonia oxidisers for nitrous oxide emissions. *ISME J* 12:1084–1093.

28. Finlayson-Pitts BJ, Pitts JN, Jr (2000) Chemistry of inorganic nitrogen compounds. *Chemistry of the Upper and Lower Atmosphere* (Academic, San Diego), pp 264–293.

29. Kleffmann J, et al. (2003) Measured and simulated vertical profiles of nitrous acid. Part I. Field measurements. *Atmos Environ* 37:2949–2955.

30. Oswald R, et al. (2015) A comparison of HONO budgets for two measurement heights at a field station within the boreal forest in Finland. *Atmos Chem Phys* 15:799–813.

31. VandenBoer TC, et al. (2013) Understanding the role of the ground surface in HONO vertical structure: High resolution vertical profiles during NACHTT-11. *J Geophys Res Atmos* 118:10155–10171.

32. Tsai C, et al. (2018) Nitrous acid formation in a snow-free wintertime polluted rural area. *Atmos Chem Phys* 18:1977–1996.

33. Oswald R, et al. (2013) HONO emissions from soil bacteria as a major source of atmospheric reactive nitrogen. *Science* 341:1233–1235.

34. Donaldson MA, Bish DL, Raff JD (2014) Soil surface acidity plays a determining role in the atmospheric-terrestrial exchange of nitrous acid. *Proc Natl Acad Sci USA* 111:18472–18477.

35. Donaldson MA, Berke AE, Raff JD (2014) Uptake of gas phase nitrous acid onto boundary layer soil surfaces. *Environ Sci Technol* 48:375–383.

36. Scharko NK, et al. (2015) Combined flux chamber and genomics approach links nitrous acid emissions to ammonia oxidizing bacteria and archaea in urban and agricultural soil. *Environ Sci Technol* 49:13825–13834.

37. Ambus P, Zechmeister-Boltenstern S, Butterbach-Bahl K (2006) Sources of nitrous oxide emitted from European forest soils. *Biogeosciences* 3:135–145.

38. Ambus P, Skiba U, Butterbach-Bahl K, Sutton MA (2011) Reactive nitrogen and greenhouse gas flux interactions in terrestrial ecosystems. *Plant Soil* 343:1–3.

39. Pajares S, Bohannan BJM (2016) Ecology of nitrogen fixing, nitrifying, and denitrifying microorganisms in tropical forest soils. *Front Microbiol* 7:1045.

40. Levy-Booth DJ, Prescott CE, Grayston SJ (2014) Microbial functional genes involved in nitrogen fixation, nitrification and denitrification in forest ecosystems. *Soil Biol Biochem* 75:11–25.

41. Hawkes CV, DeAngelis KM, Firestone MK (2007) Root interactions with soil microbial communities and processes. *The Rhizosphere*, eds Cardon Z, Whitbeck JL (Academic, Burlington, NJ), pp 1–29.

42. Phillips RP, Brzostek E, Midgley MG (2013) The mycorrhizal-associated nutrient economy: A new framework for predicting carbon-nutrient couplings in temperate forests. *New Phytol* 199:41–51.

43. Midgley MG, Phillips RP (2016) Resource stoichiometry and the biogeochemical consequences of nitrogen deposition in a mixed deciduous forest. *Ecology* 97:3369–3378.

44. Lin G, McCormack ML, Ma C, Guo D (2017) Similar below-ground carbon cycling dynamics but contrasting modes of nitrogen cycling between arbuscular mycorrhizal and ectomycorrhizal forests. *New Phytol* 213:1440–1451.

45. Vitousek PM, Matson PA (1985) Causes of delayed nitrate production in two Indiana forests. *For Sci* 31:122–131.

46. Stark JM, Hart SC (1997) High rates of nitrification and nitrate turnover in undisturbed coniferous forests. *Nature* 385:61–64.

47. Paavolainen L, Kitunen V, Smolander A (1998) Inhibition of nitrification in forest soil by monoterpenes. *Plant Soil* 205:147–154.

48. Uusitalo M, Kitunen V, Smolander A (2008) Response of C and N transformations in birch soil to coniferous resin volatiles. *Soil Biol Biochem* 40:2643–2649.

49. Liu S, et al. (2017) Abiotic conversion of extracellular NH_2OH contributes to N_2O emission during ammonia oxidation. *Environ Sci Technol* 51:13122–13132.

50. Homyak PM, et al. (2016) Aridity and plant uptake interact to make dryland soils hotspots for nitric oxide (NO) emissions. *Proc Natl Acad Sci USA* 113:E2608–E2616.

51. Dhakal P, Matocha CJ, Huggins FE, Vandiviere MM (2013) Nitrite reactivity with magnetite. *Environ Sci Technol* 47:6206–6213.

52. Heil J, Vereecken H, Brüggemann N (2016) A review of chemical reactions of nitrification intermediates and their role in nitrogen cycling and nitrogen trace gas formation in soil. *Eur J Soil Sci* 67:23–39.

53. Homyak PM, Kamiyama M, Sickman JO, Schimel JP (2017) Acidity and organic matter promote abiotic nitric oxide production in drying soils. *Glob Change Biol* 23:1735–1747.

54. Wrage-Mönnig N, et al. (2018) The role of nitrifier denitrification in the production of nitrous oxide revisited. *Soil Biol Biochem* 123:A3–A16.

55. Nelson DW, Bremner JM (1970) Gaseous products of nitrite decomposition in soils. *Soil Biol Biochem* 2:203–204.

56. Prather RJ, Miyamoto S (1974) Nitric oxide sorption by calcareous soils. III. Effects of temperature and lack of oxygen on capacity and Rate1. *Soil Sci Soc Am J* 38:582–585.

57. Slemr F, Seiler W (1984) Field measurements of NO and NO_2 emissions from fertilized and unfertilized soils. *J Atmos Chem* 2:1–24.

58. Slemr F, Seiler W (1991) Field study of environmental variables controlling the NO emissions from soil and the NO compensation point. *J Geophys Res* 96:13017–13031.

59. Williams EJ, Hutchinson GL, Fehsenfeld FC (1992) NO_x and N_2O emissions from soil. *Global Biogeochem Cycles* 6:351–388.

60. Reed C, et al. (2016) HONO measurement by differential photolysis. *Atmos Meas Tech* 9:2483–2495.

61. Kebede MA, Bish DL, Losovyj Y, Engelhard MH, Raff JD (2016) The role of iron-bearing minerals in NO_2 to HONO conversion on soil surfaces. *Environ Sci Technol* 50:8649–8660.

62. Scharko NK, Martin ET, Losovyj Y, Peters DG, Raff JD (2017) Evidence for quinone redox chemistry mediating daytime and nighttime NO_2-to-HONO conversion on soil surfaces. *Environ Sci Technol* 51:9633–9643.

63. Yan X, Ohara T, Akimoto H (2005) Statistical modeling of global soil NO_x emissions. *Global Biogeochem Cycles* 19:GB3019.

64. Venterea RT, et al. (2004) Soil emissions of nitric oxide in two forest watersheds subjected to elevated N inputs. *For Ecol Manage* 196:335–349.

65. Fitzhugh RD, Lovett GM, Venterea RT (2003) Biotic and abiotic immobilization of ammonium, nitrite, and nitrate in soils developed under different tree species in the Catskill Mountains, New York, USA. *Glob Change Biol* 9:1591–1601.

66. Pilegaard K, et al. (2006) Factors controlling regional differences in forest soil emission of nitrogen oxides (NO and N_2O). *Biogeosciences* 3:651–661.

67. National Atmospheric Deposition Program (2016) Total deposition 2015 annual map summary. NADP data report 2016-02 (University of Illinois, Urbana-Champaign, IL).

68. Averill C, Dietze MC, Bhatnagar JM (2018) Continental-scale nitrogen pollution is shifting forest mycorrhizal associations and soil carbon stocks. *Glob Change Biol* 24:4544–4553.

69. Lamsal LN, et al. (2015) U.S. NO_2 trends (2005–2013): EPA Air Quality System (AQS) data versus improved observations from the Ozone Monitoring Instrument (OMI). *Atmos Environ* 110:130–143.

70. van Kessel MA, et al. (2015) Complete nitrification by a single microorganism. *Nature* 528:555–559.

71. Taylor AE, Zeglin LH, Wanzek TA, Myrold DD, Bottomley PJ (2012) Dynamics of ammonia-oxidizing archaea and bacteria populations and contributions to soil nitrification potentials. *ISME J* 6:2024–2032.